



XN9600151

Stability Of Thermally Induced Copper Precipitates Under Neutron Irradiation.

W.J. Phythian, S.Dumbill, P.Brown and R. Sinclair

AEA Technology, Harwell Laboratory
Didcot, Oxfordshire, OX11 0RA, UK

Abstract

It is well known that copper precipitation plays a key role in the degradation of mechanical properties of irradiated Reactor Pressure Vessel (RPV) steels. Depending on the thermo mechanical treatment of the steel and the irradiation conditions experienced, a range of copper precipitate size and number densities can be produced. Generally, in high copper welds (>0.3wt% Cu), typical post weld heat treatments produce stable copper precipitates ~10nm diameter. The remaining copper in solution has the potential to precipitate out under irradiation, forming coherent precipitates ~2nm in diameter, similar in size to those found in thermally aged samples in the peak hardness condition. The factors controlling the nucleation, growth and stability of copper precipitates under irradiation is therefore of importance to understanding the materials behaviour.

Model Fe 1.3%Cu and Fe 1.3%Cu 1.1%Ni alloys have been thermally aged at 550°C for 2hrs (peak) and 10hrs prior to irradiation at 288°C to a dose of 5.10^{22} n/m². Results of a microstructural investigation using dedicated field emission gun scanning transmission electron microscopy (FEGSTEM) and small angle neutron scattering (SANS) to assess precipitate stability in the binary alloy will be presented. These data are then used to predict a hardness change as a result of copper precipitation for comparison with the measured values obtained using standard 5kg Vickers hardness tests on the SANS samples. The implications of these data to the reembrittlement of the RPV by subsequent copper precipitation will be discussed.

1 Introduction

This paper describes the preliminary results from an experimental programme set up to establish the stability of copper precipitates formed during post weld heat treatment or vessel annealing in plant life extension programmes. Copper is known to

precipitate out of solution under thermal or irradiation conditions and the resultant precipitates form efficient barriers to dislocation motion with a resultant increase in hardness and subsequent embrittlement. Under irradiation the copper available to precipitate in this way may not necessarily be the same as the bulk level. In high copper welds, post weld heat treatment (PWHT) can remove copper from the matrix forming copper precipitates that generally are observed as ~10nm diameter 'foc' precipitates associated with dislocations. In welds, further copper can be removed as a result of copper sulphide formation. In practice this reduces to the following equation:

$$Cu_{matrix} = Cu_{bulk} - Cu_S - Cu_{HT\ ppt} - Cu_{Irrad\ ppt}$$

Cu_S = Copper associated with sulphur in the form of copper sulphide

$Cu_{HT\ ppt}$ = Copper in the form of large foc copper precipitates formed during post-weld heat -treatment.

$Cu_{Irrad\ ppt}$ = Copper in the form of small bcc precipitates formed under irradiation.

A measure of copper precipitation therefore requires knowledge of the copper matrix value and the development of techniques to measure this critical parameter either directly or indirectly.

In plant life extension, various annealing options are being considered that will remove the hardening effect of the small copper precipitates by thermally treating to permit these precipitates to grow into the less harmful incoherent precipitates, similar to those produced in PWHT or found in overaged model alloys. It is the stability of these large precipitates under irradiation or reirradiation that is of interest to this study as, if they subsequently dissolve under irradiation, they will act as a source of Cu for subsequent fine scale precipitation resulting in increased hardness.

Under irradiation the precipitates formed are similar in size to those generated at peak hardness in thermal ageing experiments. The microstructural investigations conducted on this and other irradiated material suggest that the irradiation induced precipitates remain small, with a coherent bcc structure, and that no overageing takes place in the irradiated material.

With this as background information, a series of experiments were set up to examine the effect of irradiation on the size and number density of precipitates. Samples were heat treated to produce two types of precipitate, namely small coherent precipitates found at peak hardness and those found in the overaged condition. In addition to this material, as quenched samples with all the copper in solution were included as controls. Samples were examined by both electron microscopy techniques and small angle neutron scattering (SANS) to assess the distribution of copper (matrix or precipitate) and to determine the size and number density of precipitates formed under thermal or irradiation conditions.

2 Material and Irradiation conditions

Binary Fe - 1.3wt% Cu alloy, HE, used in previous studies [1] has been employed here. Samples were given a solution heat treatment of 825°C for 6hrs followed by a water quench (HEQ). Further ageing at 550°C produced a peak in hardness after two hours (HE2), with subsequent overaging after ten hours to produce sample HE10.

All samples were irradiated in the PLUTO MTR at Harwell as part of a major programme of irradiations. The 1154 instrumented rig employed gas mixture and gas gap techniques to maintain the temperature of the sample carrier. Temperatures were monitored throughout by thermocouples with an average recorded temperature of 290±8°C being attained by all the samples. Six sample carriers were loaded to attain a range of doses between 0.1 and 3×10²³ n/m² (E>1MeV). However, as a result of the rescheduling of reactor operations and the ultimate closure of the facility, only three out of the six capsules were irradiated. The irradiated samples examined in this study received a dose of 0.53×10²³ n/m² (E>1MeV) at a dose rate of 46±10×10¹⁶ n/m²/sec. The samples are prefixed with 'I' to denote irradiated in future text.

3 Results

3.1 Hardness results

Hardness values were obtained by conventional Vickers hardness testing using 5kg loads, with three indents being performed on each sample. These tests were performed on samples used in the SANS investigations. Samples were 1mm

thick and of diameter between 8 and 9 mm. The results of this testing are shown in Table 1 and graphically in figure 1. Examination of the figure, clearly shows the significant rise in hardness from both thermally aged material peaking at 2 hrs. The increase in hardness for all the irradiated material above the starting condition is clearly visible, the effect being strongest in the as quenched condition (IHEQ).

Table 1
Hardness values of thermally aged and irradiated samples

| Sample Number | Hardness (1σ) | Change due to thermal ageing | Change due to Irradiation |
|---------------|---------------|------------------------------|---------------------------|
| HEQ | 95 ± 2 | 0 | |
| IHEQ | 238 ± 5 | | 143 ± 5 |
| HE2 | 189 ± 2 | 94 ± 3 | |
| IHE2 | 221 ± 7 | | 32 ± 7 |
| HE10 | 170 ± 3 | 75 ± 4 | |
| IHE10 | 204 ± 3 | | 34 ± 4 |

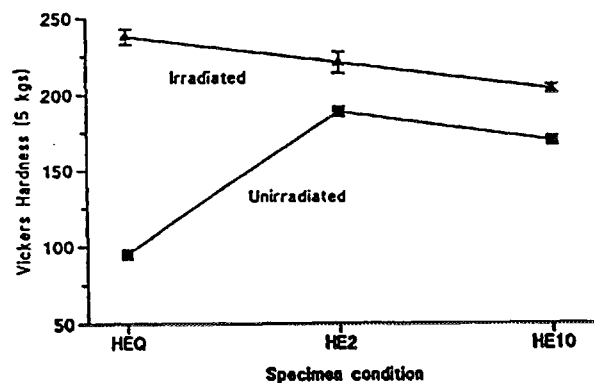


Figure 1 Hardness measurements of the thermally aged and irradiated samples.

3.2 Microstructural examination

Three types of microstructural examination were performed. The first using TEM, was employed to examine for any large scale changes in microstructure and to determine size distribution data, in particular for the larger precipitates to act as an independent check on the SANS data, this comparison when complete will be presented elsewhere. FEGSTEM was used to determine copper matrix levels and to establish the volume fraction of copper in the form of small precipitates. Again this data can be used to independently confirm the data produced by SANS.

3.2.1 STEM Technique and Results

Since our earlier work on these alloys [1,2], the first to use dedicated FEGSTEM examinations on this class of material, considerable advances have been made [3-5]. These concern both advances in equipment such as the use of Parallel Electron Energy Loss Spectroscopy, and in the methodology of the analysis, eg the use of spot and area scan modes. The use of PEELS in the study of RPV steel microstructures has two benefits, namely the ability to analyse for Mn in the precipitates,[3-6] and using the annular detector to image small precipitates by changes in atomic weight (Z contrast). These samples have been examined throughout this technique evolution and so are useful indicators of the techniques capabilities.

By conducting analysis in the FEGSTEM, an instrument capable of producing high intensity electron beams some 2nm diameter, chemical analysis with nm spatial accuracy can be obtained by Energy Dispersive X-ray analysis (EDX). The technique employed for matrix copper determination was to position the beam in precipitate free regions of the foil, as assessed by imaging using Z contrast, and collecting the signal until a set number of counts or acquisition time had been obtained. These spectra were then analysed using commercial 'Link' software to produce composition values. The process was repeated several times depending upon the accuracy required and the amount of spatial variation in the sample.

The sample is held in a specially modified holder which is of copper-free construction thus eliminating any copper signal arising from beam/holder interactions. Calibration checks with an Fe sample have shown that the background copper level after a 300 second acquisition time spectrum is unresolvable and is therefore considered to be <0.05%. The quoted values have therefore not be adjusted for any background copper effects.

The errors on the analysis can be split into two components, those from the analysis technique, considered for Cu to be ± 0.02 , and those arising from spatial inhomogeneity of the sample at the nm level due to ultrafine precipitates etc. The latter can produce differences in spectra to a maximum of ~ 0.2 wt%. It is these errors that can be minimised by conducting more analysis under well defined conditions, eg variation in foil thickness, knowledge of beam drift etc., and application of statistical methods to deconvolute the measured distribution of spectra to obtain appropriate matrix values.

As an indicative guide, for 5 matrix spot mode values we would not expect an accuracy of better than $\sim \pm 0.1$, while 15 to 20 values now typically produces an error of $\sim \pm 0.03$. However, this latter technique requires foil thickness information readily obtainable from PEELS, not fully developed at the time of making the STEM measurements reported here and is reflected in the accuracy of the data. Even so the data have improved over

previous reported work [1] on this alloy and are comparable with accuracy inferred from other techniques such as SANS, making comparisons possible between the two techniques. Data from small area scans and large area scans provide valuable information on the distribution of copper in the form of small and large precipitates. The large area scan can be compared to bulk values directly, while the difference between large and small can be related to the volume fraction of large copper precipitates.

Differences between the spot and small area scan modes can therefore be used to assess the volume fraction of copper associated with small precipitates. The positioning of the spot and small area scan is shown by the crosses and boxes in figure 2. The large area scan would typically cover an area the size of the micrograph. This figure was obtained on the STEM from sample IHE10 using Z contrast, here the precipitates appear as white spots. Examination of the figure shows a bimodal distribution in precipitate size, both small $\sim 2-5$ nm diameter and larger ~ 10 nm precipitates can be seen.

In developing the technique, one deficiency of the above is manifest by comparison of the data produced by large area scans compared with a bulk value of 1.3wt%. In all cases the large area scans under predict the bulk value, the effect being strongest in the thermally aged material. We have now attributed this to the preferential leaching out of the foil, in the electropolishing process, those large copper precipitates intersecting the surface, thereby reducing the copper level measured in the scan. This loss of large copper precipitates does not affect the small area scan and spot mode measurements as these are positioned to avoid any large precipitates.

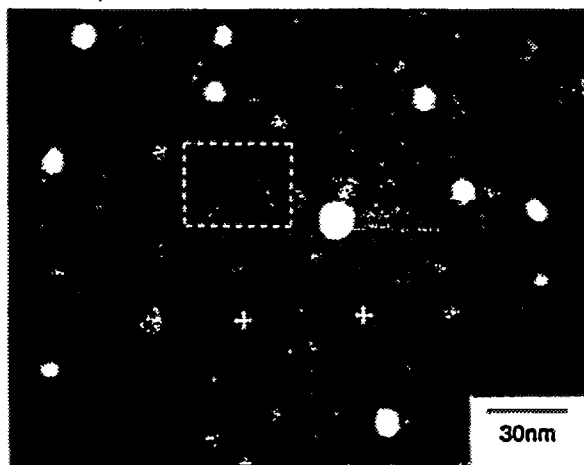


Figure 2 Polaroid image obtained from the FEGSTEM on sample IHE10, the image was produced using Z contrast. The precipitates appear as white spots. The spot, small area and large area scans are represented by crosses, dotted box and the whole micrograph respectively.

The results of the STEM analysis are shown graphically in figure 3. The figure show the histograms for spot, small and large area scan. From these values average data were calculated and are shown in Table 2

Table 2
Measured copper concentrations (wt%) as determined by STEM

| | Spot | Small Area | Large Area |
|-------|-----------|------------|------------|
| HEQ | 1.26±0.08 | 1.32±0.06 | 1.28±0.03 |
| IHEQ | 0.15±0.09 | * | 1.21±0.02 |
| HE2 | 0.40±0.04 | 0.92±0.13 | 1.07±0.07 |
| IHE2 | 0.19±0.05 | 0.86±0.03 | 1.20±0.04 |
| HE10 | 0.32±0.04 | 0.49±0.06 | 1.05±0.09 |
| IHE10 | 0.17±0.08 | 0.30±0.01 | 1.17±0.05 |

* Not measured - assume same as large area value

3.2.2 SANS Results

SANS experiments were made with the SANS instrument in the neutron guide house of the DR3 reactor, Risø, Denmark. The measurements were made using a wavelength of 0.6nm and sample to detector distances of 1.25 and 2.5m to cover the required scattering vector (Q) range. In addition to the samples, a calibration sample of water (1mm thick) and backgrounds were measured at both detector positions. The PLUTO-SANS electromagnet was installed in the sample vacuum enclosure of the instrument to provide the required 1T field for magnetic measurements. These measurements are necessary to produce A ratio values and hence compositional information on the precipitates in addition to the size and number density values. Figure 4 shows intensity versus Q^2 plots in zero field. This data together with that obtained in magnetic field has been processed using the maximum entropy methods^[6,7] employed by Buswell et al^[1], to produce the precipitate size distribution plots presented in figure 5. The figures, for clarity, show line diagrams taken at the mid point of the histogram bin. The fine structure observed in the distribution is an artefact of the maximum entropy technique and the bin width chosen for display. The volume fraction information is derived independently and not subject to such choice of bin width.

The SANS data are summarised for all the conditions examined in Table 3. The table presents both diameter (d), volume fraction (V_f) and number density (N_d) values for the total population, for the small coherent bcc precipitates ($d < 6nm$) and the large incoherent precipitates ($d > 6nm$). The choice of 6nm is in keeping with previous work on this alloy and permits comparisons to be made. The precise transition from bcc to 'fcc' is not well

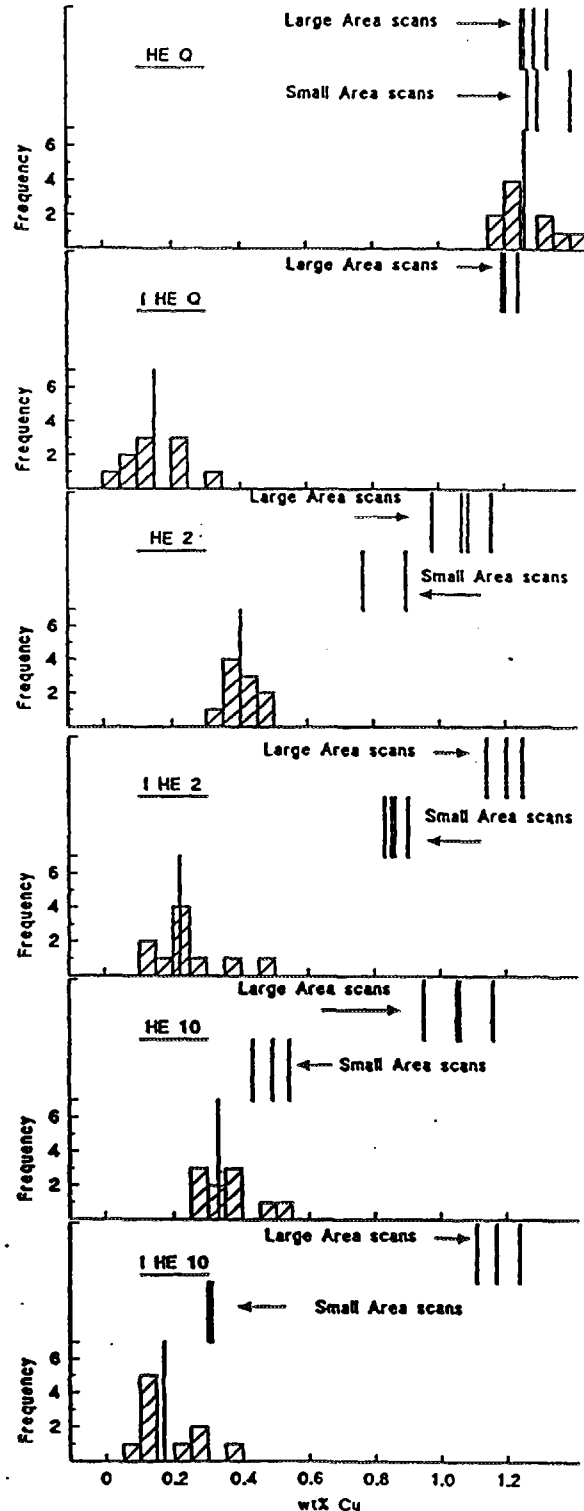


Figure 3 Copper determination from FEGSTEM analysis. The data show the values obtained in spot, small area and large area scan modes.

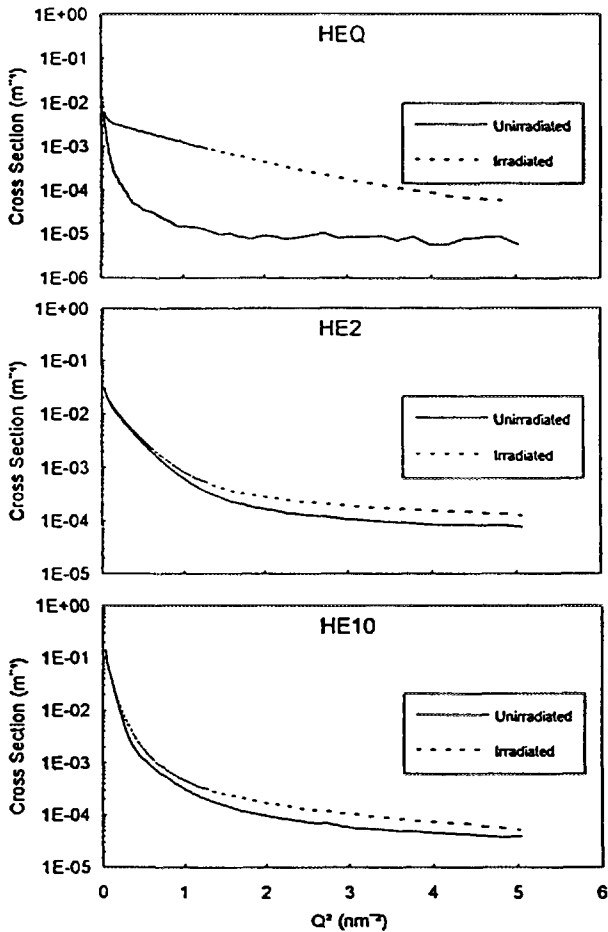


Figure 4 Differential scattering cross sections as a function of Q^2 for unirradiated and irradiated HEQ, HE2 and HE10.

Table 3 Summary of SANS data

| Sample | A ratio | Assumed Precipitate Composition (at%) | All precipitates | | | | | bcc precipitates (d=6nm) | | | fcc precipitates (d=6nm) | | | Residual Matrix Cu (wt%) | STEM matrix Cu (wt%) |
|--------|---------|---------------------------------------|--------------------------------------|-----------------------|------------------------|--------------------------------|---------------------------------|--------------------------|---------------------|--------------------------------|--------------------------|---------------------|--------------------------------|--------------------------|----------------------|
| | | | Average Feature Diam.(nm $\pm 5\%$) | Ppt Vol. Fraction (%) | Void Vol. Fraction (%) | Ppt Num. Density $10^{23}/m^3$ | Void Num. Density $10^{23}/m^3$ | Diameter (nm) | Volume Fraction (%) | Ppt Num. Density $10^{23}/m^3$ | Diameter (nm) | Volume Fraction (%) | Ppt Num. Density $10^{23}/m^3$ | | |
| HEQ | | | 1.8 | | | | | | | | | | | | 1.3 |
| IHEQ | 11.1 | 100Cu 96Cu4vac 100Cu+voids | 3.7 | 0.82 0.78 0.95 | | 3.10 2.94 3.59 | | | | | | | | 0.3 0.4 0.2 | 0.2 |
| HE2 | n/a | 100Cu 96Cu4vac 100Cu+voids | 5.5 | 0.85 0.81 0.78 | -0.03 | 0.98 0.93 0.89 | | 2 2 | 0.26 0.25 | 6.18 5.90 | 7 | 0.59 0.57 | 0.34 0.32 | 0.3 0.3 0.3 | 0.4 |
| IHE2 | 7.5 | 100Cu 96Cu4vac 100Cu+voids | 4.7 | 1.21 1.15 0.88 | 0.02 | 2.22 2.11 1.62 | 0.14 | 2 | 0.55 0.53 | 13.18 12.56 | 7 | 0.65 0.62 | 0.36 0.35 | 0.0 0.0 0.3 | 0.2 |
| HE10 | n/a | 100Cu 96Cu4vac 100Cu+voids | 12.3 | 1.03 0.98 0.94 | 0.02 | 0.11 0.10 0.10 | 0.00 | 1.5 | 0.14 0.14 | 8.04 7.64 | 14 | 0.89 0.85 | 0.06 0.06 | 0.1 0.2 0.2 | 0.3 |
| IHE10 | 8.7 | 100Cu 96Cu4vac 100Cu+voids | 10.1 | 1.10 1.05 0.97 | 0.03 | 0.20 0.20 0.18 | 0.01 | 2.2 | 0.21 0.20 | 3.75 3.57 | 12 | 0.90 0.85 | 0.10 0.09 | 0.1 0.1 0.2 | 0.2 |

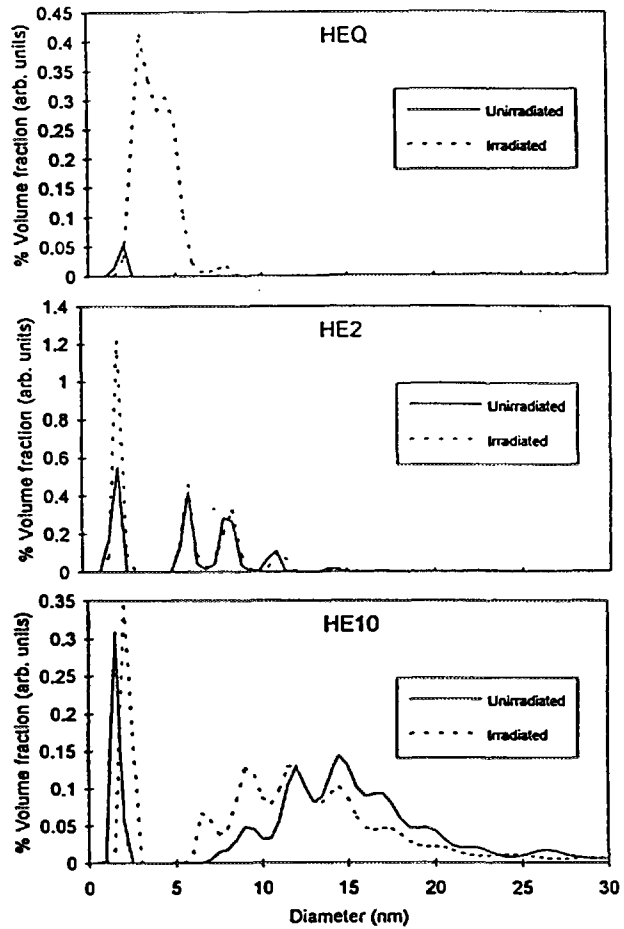


Figure 5 Volume weighted particle size distributions obtained for unirradiated and irradiated HEQ, HE2 and HE10. The lines join the centre of histogram bins and therefore the fine structure is an artefact of the choice of bin size and the maximum entropy method.

defined and is the subject of ongoing research activities^[8-10]. The absolute volume fraction is dependant upon the assumed precipitate composition, the table gives some alternatives, e.g. 100%Cu, a copper 4% vacancy alloy and a mixture of pure copper precipitates and microvoids having identical size distributions. In addition, from a knowledge of the volume fraction of precipitate and starting copper available for precipitation, it is possible to calculate the copper remaining in the matrix, these values are shown together with those obtained by direct measurement with FEGSTEM.

4 Discussion

4.1 Copper precipitation

The data obtained in this study are in excellent agreement with earlier studies on thermal ageing (550°C) experiments using this alloy. Both studies confirm a rise in hardness to a peak at approximately 2hrs, with overageing and associated reduction in hardness being observed in the 10hr condition. Microstructural analysis confirms that for conditions of peak hardness, not all the copper has been removed from solution. Analysis by SANS and by the differencing techniques adopted in the FEGSTEM, confirm a large volume fraction of small precipitates are present. Further analysis also reveals a population of larger $d > 6\text{nm}$ are also present, but with a considerably lower number density.

Under irradiation, the population of small precipitates is enhanced, the effect being the most dramatic in the HEQ sample where all the copper was available for precipitation at the start of the irradiation. In other samples where copper matrix values were lower at the start of the irradiation, the incremental hardness associated with irradiation is smaller. In all the irradiated alloys, the final copper matrix value measured by FEGSTEM is similar, with an average of 0.17 wt%, indicating that full precipitation has not yet been achieved under these irradiation conditions, i.e. not yet achieved full depletion of the matrix copper. This is in keeping with our earlier work and will be discussed in detail elsewhere.

Comparison of the two techniques employed to determine volume fraction of copper precipitate is shown in Table 4. In general the agreement is very good, given the uncertainties of the measuring methods and the assumptions employed, e.g. that the precipitate composition is 100% copper. Further work is required on sample HE2 to determine the source of the difference between the two techniques, but the initial assessment points to the arbitrary split of small and large precipitates at 6nm in the SANS data. A repeat STEM examination is planned, using a sample cut from the SANS specimen examined as part of this study.

Table 4

Comparison of measured precipitate volume fractions

| Sample | Volume Fraction (at%) | | | |
|--------|-----------------------|------------------------|-------------------|-------------------|
| | FEGSTEM | | SANS | |
| | S/A - Spot | L/A -S/A (Bulk-S/A) | $d < 6\text{ nm}$ | $d > 6\text{ nm}$ |
| HE2 | 0.46 | 0.01(0.19) | 0.26 | 0.59 |
| HE10 | 0.15 | 0.49(0.71) | 0.14 | 0.88 |
| IHEQ | 0.93 | N/A | 0.88 | N/A |
| IHE2 | 0.59 | 0.29(0.38) | 0.55 | 0.65 |
| IHE10 | 0.11 | 0.76(0.88) | 0.14 | 0.89 |

4.2 Effect of irradiation on precipitates

The size of the thermally aged and irradiation induced precipitates is in agreement with previous studies on these alloys^[1]. However, the effect of irradiation on existing precipitates has not been previously examined, although the good agreement obtained does give confidence to the accuracy of this new data. Under irradiation the SANS data suggests that the size of the small precipitates induced at peak hardness remain relatively unchanged, but increase in number. The larger precipitates in the overaged sample HE10 apparently undergo a reduction in mean size from 14 to 12 nm, however, the volume fraction of precipitate ($d > 6\text{nm}$) remains constant as a result of increase in number density of the smaller precipitates in this size distribution.

In welds, microstructural examination shows that the precipitates produced in PWHT are typically 10 to 20nm diameter, and under the irradiation conditions experienced by the vessel are essentially unchanged, as measured qualitatively by TEM in unirradiated and irradiated material. Quantitative information on the large precipitates in commercial material is not available. SANS studies generally are concerned with the small precipitates, and in typical commercial material with copper values above ~0.3, little information exists in the open literature. As the bulk copper levels are not as high as the model alloys employed here, even if SANS data were available, the volume fraction of large precipitates is relatively small, making any comments on the change in this part of the SANS signal statistically invalid.

A better opportunity for comparison comes from work on irradiated, annealed and reirradiated material, where a high percentage of the copper during the annealing stage is in the form of large precipitates. Again the only SANS analysis of such material in the open literature is the data of Kampmann et al^[11] that unfortunately does not permit comparisons of the large precipitate distribution to be made due to the use of total volume fraction and size information, i.e. the presence of a bimodal distribution is acknowledged but not analysed in terms of the two components that make up the overall distribution.

It is therefore extremely difficult to rationalise these observations of precipitate refinement with observed effects in commercial-type material. The applicability of the model alloy with extremely high, by RPV standards, copper content and the extremely high dose rates of the irradiation need to be considered before over interpretation of the data to suggest that large copper precipitates in RPV welds are unstable under irradiation. It is thought that the data are more relevant to plant life extension studies employing annealing, as not only will the time and temperature of the anneal affect precipitate size and hence stability under subsequent irradiation, but the surrounding microstructure will be considerably cleaner than in the as fabricated condition. This 'clean' microstructure local to the precipitate will therefore be more like that observed in the model alloys examined in this study. It may therefore explain the rapid re embrittlement observed in high copper material^[12] after annealing. Here the rate of embrittlement is close to that observed at start of life condition, even though matrix copper values should be considerably lower in the annealed material. Microstructural examination of this material to provide matrix copper values would be required to understand further the role of annealing and the subsequent response of the material to irradiation.

4.3 Mechanical properties from microstructural data

The volume fraction and size information can be used in combination with the Russell-Brown^[13] modulus hardening theory to predict yield strength and subsequent hardness change. The data have been calculated in accordance with Phythian et al^[2] using the modulus values for bcc copper. This has been done for all the conditions examined using the size information from SANS, and the volume fraction information is that generated for the small precipitates $d < 6\text{nm}$ by SANS and the small area - spot mode differencing technique developed for FEGSTEM. The information on the large precipitates has not been used as these incoherent precipitates harden by a different mechanism where use of the modulus hardening theory is not appropriate. The hardness data and volume fraction information used in the analysis are presented in Table 5.

The data predict hardness changes associated with bcc copper precipitates making a direct comparison with experimental data difficult especially so in the irradiated material where in addition to copper precipitation, matrix damage (loops and/or microvoids) are formed. The copper contribution is in keeping with the values predicted for this irradiation condition by models of embrittlement^[14-16]. To determine the partitioning of the observed hardness into these two components, a series of post irradiation annealing experiments are now underway and will be reported elsewhere. When available these should act as further

Table 5

Comparison of experimental hardness data with predicted values using microstructural volume fraction data and modulus hardening theory.

| Sample | Change in Hardness | Volume fraction of precipitate (at%) | | Mean ppt Diameter (nm) | Calculated hardness from precipitate Russell-Brown | |
|--------|--------------------|--------------------------------------|------|------------------------|--|------|
| | | STEM | SANS | | STEM | SANS |
| HEQ | 0 | 0 | 0 | 0 | 0 | 0 |
| HE2 | 94 | 0.46 | 0.26 | 2 | 87 | 65 |
| HE10 | 75 | 0.15 | 0.14 | 1.5 | 33 | 33 |
| IHEQ | 143 | 0.93 | 0.82 | 3.7 | 121 | 114 |
| IHE2 | 126 | 0.59 | 0.55 | 2 | 98 | 95 |
| IHE10 | 109 | 0.11 | 0.14 | 2.2 | 44 | 61 |

independent checks on the validity of the Russell-Brown model for this type of work. For the unirradiated samples, the only appropriate comparison with experiment is the change in hardness between HEQ and HE2, here the experimental value of 94 is in good agreement with that predicted from microstructural data. Values of 87 and 65 are predicted when using the FEGSTEM and SANS volume fractions respectively, giving further support to the use of the differencing technique employed with the FEGSTEM data.

The observed increase in hardness between the unirradiated and irradiated HE10 can be explained by the increase in both the number density and mean size of the small coherent precipitates observed in this alloy. Application of the R-B model to this data predicts an increase in hardness between 22 to 34Hv depending upon the size of precipitate used (1.5 or 2.2nm), this compares well with the measured increase of 34Hv that also includes a contribution from matrix defects. The change in the size distribution for the larger precipitates is of importance to understanding the effects of PWHT and re-embrittlement after annealing. The data for HE10 suggest that under irradiation a new equilibrium position is set up where the mean precipitate size is smaller than that observed under thermal conditions alone.

5 Conclusions

Techniques have been developed to assess directly and indirectly the copper remaining in the matrix as a result of thermal or irradiation induced precipitation.

In general good agreement is achieved between the two techniques for precipitate volume fraction assessment.

Modelling the hardness change can be successfully accomplished using the modulus hardening theory and appropriate bcc modulus data.

Thermal ageing produces a range of precipitate sizes, the peak occurring in this model alloy after 2hrs at 550°C. In this condition, the matrix is not depleted of copper, peak hardness being achieved by the optimum number and size of bcc precipitates. Overageing results in an increase in precipitate size and relatively modest increase in precipitate volume fraction.

Irradiation of the material independent of the starting copper matrix results in a similar matrix depletion of copper under irradiation. The irradiation condition examined here does not appear to have reached peak hardness, with ~0.17wt% remaining in solution.

The size and number density of larger ($d > 6\text{nm}$) is refined by irradiation, bringing average diameters down from 14 to 12nm, with associated increase in the number density of precipitates at the smaller end of this distribution. The net result is a relatively constant volume fraction of precipitate.

Acknowledgements

This work was funded as part of the Corporate Investment Programme of AEA Technology under grant 92-1049. The SANS facility at Risø received financial support from the Large Installation Programme of CEC. The authors would like to thank K. Mortensen and his staff at the Risø National Laboratory, Denmark, for assistance with the SANS experiments.

REFERENCES

- 1 J.T. Buswell, C.A. English, M.G. Hetherington, W.J. Phythian, G.D.W. Smith and G.M. Worrall, *Effects of Radiation on Materials: 14th International Symposium (Volume II)*, (ASTM STP 1046, Philadelphia, 1990) p.127
- 2 W.J. Phythian, A.J.E. Foreman, C.A. English, J.T. Buswell, M. Hetherington, K. Roberts and S. Pizzini, *Effects of Radiation on Materials: 15th International Symposium, Nashville 1990*. (ASTM STP 1127, 1992)
- 3 W.J. Phythian, N. De Diego, J. Mace and R.J. McElroy, *Proc. 16th Int. Symp. on Effects of Radiation on Materials, Denver, USA 1992*. To be published as ASTM STP 1175.
- 4 J.T. Buswell, C.J. Bolton, M.R. Wootton, P.J.E. Bischler, R.B. Jones, W.J. Phythian and R.N. Sinclair, *Proc. 16th Int. Symp. on Effects of Radiation on Materials, Denver, USA 1992*. To be published as ASTM STP 1175.
- 5 W.J. Phythian and C.A. English. *Proc of Int. Conf. 'Microstructural Evolution in Irradiated Materials'*, Muskoka, Canada. Sept 1992, To be published in *J. Nucl. Materials*, 1993.
- 6 J.A. Pouton, G.J. Daniell and B.D. Rainford, *J. Appl. Cryst.* 21, (1988) 663
- 7 J.A. Pouton, G.J. Daniell and B.D. Rainford, *J. Appl. Cryst.* 21, (1988) 891
- 8 P.J. Othen, M.L. Jenkins, G.D.W. Smith and W.J. Phythian. *Phil. Mag. Letts* 64, (1991) 383
- 9 P.J. Othen, M.L. Jenkins and G.D.W. Smith, To be published in *Proc. Int. Conf. Martensitic Transformations*, (Monterey, California June 1991)
- 10 S.Pizzini, K.J. Roberts, W.J. Phythian, C.A. English and G.N. Greaves, *Phil. Mag. Letters* 61, (1990) 223
- 11 R. Kampmann, F. Frisius, H. Hackbarth, P.A. Beavan, R. Wagner and J.R. Hawthorne. *Proceedings of 5th Int.Sym. on Environmental Degradation of Materials in Nuclear Power Systems-Water Reactors*. Monterey, California 1991 (ANS Order No 700176, 1992).
- 12 J.R. Hawthorne and A.L. Hiser. *Proceedings of 5th Int.Sym. on Environmental Degradation of Materials in Nuclear Power Systems-Water Reactors*. Monterey, California 1991 (ANS Order No 700176, 1992).
- 13 K.C. Russell and L.M. Brown, *Acta. Met.* 20, (1972) 969
- 14 S.B. Fisher and J.T. Buswell, *Int. J. Pres. Ves. & Piping*, 27, (1987) 91
- 15 T.J. Williams, P.R. Burch, C.A. English and P.H.N. Ray. *Proc. 3rd Int. Symp. on Environmental Degradation of Materials in Nuclear Power Systems - Water Reactors*. Traverse City, July 1987. (The Metallurgical Society, Vol 121, 1988)
- 16 G.R. Odette and G.E. Lucas, *Proceedings of IAEA Specialists' Meeting on Irradiation Embrittlement*, Vienna, Austria, October 1984, (ASTM, 1985).